Precipitation Recycling Variability and Ecoclimatological Stability—A Study Using NARR Data. Part II: North American Monsoon Region

FRANCINA DOMINGUEZ* AND PRAVEEN KUMAR

Environmental Hydrology and Hydraulic Engineering, Department of Civil and Environmental Engineering, University of Illinois at Urbana–Champaign, Urbana, Illinois

ENRIQUE R. VIVONI

Department of Earth and Environmental Science, New Mexico Institute of Mining and Technology, Socorro, New Mexico

(Manuscript received 7 November 2006, in final form 30 January 2008)

ABSTRACT

This work studies precipitation recycling as part of the dynamic North American monsoon system (NAMS) to understand how moisture and energy fluxes modulate recycling variability at the daily-to-intraseasonal time scale. A set of land–atmosphere variables derived from North American Regional Reanalysis (NARR) data are used to represent the hydroclimatology of the monsoon. The recycling ratio is estimated using the Dynamic Recycling Model, which provides recycling estimates at the daily time scales. Multichannel singular spectrum analysis (M-SSA) is used to extract trends in the data while at the same time selecting only the variability common to all of the variables.

The 1985–2006 climatological analysis of NAMS precipitation recycling reveals a positive feedback mechanism between monsoon precipitation and subsequent increase in precipitation of recycled origin. Recycling ratios during the monsoon are consistently above 15% and can be as high as 25%. While monsoon precipitation and evapotranspiration are predominantly located in the seasonally dry tropical forests in the southwestern part of the domain, recycling is enhanced northeast of this region, indicating a relocation of soil moisture farther inland to drier regions in the northeast. The three years with the longest monsoons in the 22-yr period present an asynchronous pattern between precipitation and recycling ratio. The longest monsoons have a characteristic double peak in precipitation, with enhanced recycling ratios during the intermediate dry period. This indicates that, even when large-scale moisture advection decreases, evapotranspiration provides moisture to the overlying atmosphere, contributing to precipitation. Through the negative feedback present during long monsoons and by relocation of soil moisture, precipitation recycling brings favorable conditions for vegetation sustenance in the NAMS region.

1. Introduction

The onset of the North American monsoon system (NAMS) abruptly changes the hydroclimatology of a large region extending from northwestern Mexico to the southwestern United States (see Fig. 1). The summer season over this region is characterized by a reversal in circulation, as the midtropospheric winds shift from westerly to easterly due to the northward displacement of the subtropical ridge (Douglas et al. 1993). The circulation reversal is accompanied by an abrupt increase in precipitation. As early as May, intense rainfall begins over southern Mexico and, by July, the NAMS has migrated north into Arizona and New Mexico (Douglas et al. 1993). Most of the moisture at upper levels originates in the Gulf of Mexico and enters the region from the east, while lower-level moisture of oceanic sources originates predominantly from the tropical Pacific Ocean and the Gulf of California (Schmitz and Mullen 1996; Adams and Comrie 1997; Higgins et al. 2003). Much like the larger South Asian monsoon, the North American system is characterized by seasonal heating of the land surface lowlands and elevated areas (Tang and Reiter 1984; Adams and

* Current affiliation: Department of Hydrology and Water Resources, The University of Arizona, Tucson, Arizona.

Corresponding author address: Praveen Kumar, Environmental Hydrology and Hydraulic Engineering, Department of Civil and Environmental Engineering, University of Illinois at Urbana–Champaign, 205 N. Mathews Ave., Urbana, IL 61801.
E-mail: kumar1@uiuc.edu

DOI: 10.1175/2008JCLI1760.1

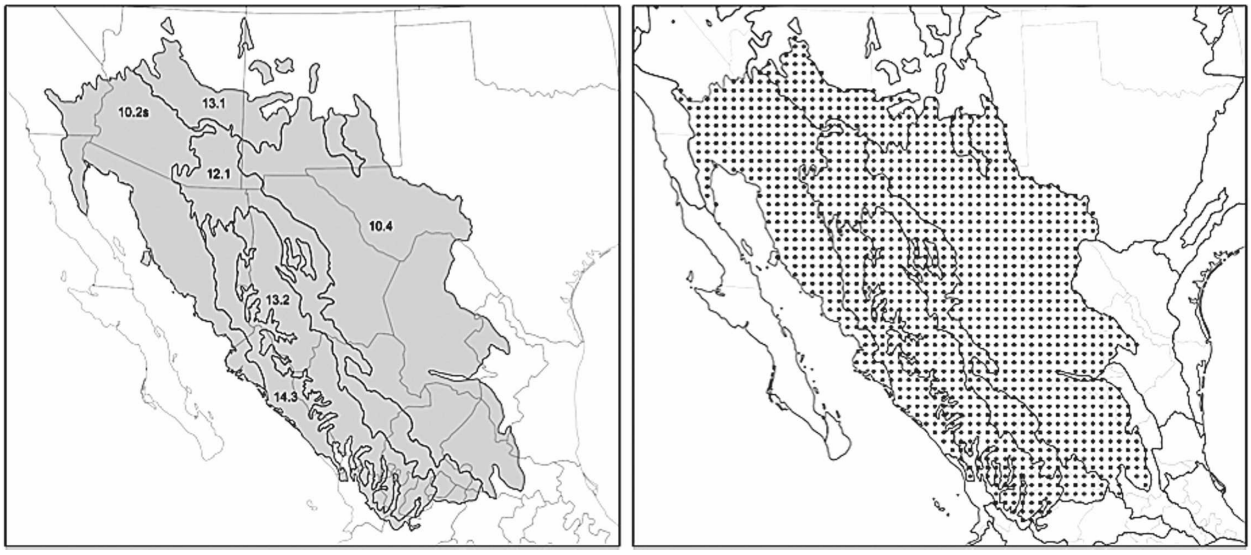

FIG. 1. (left) North American monsoon system domain, identified through six different Level II ecoregions (CEC 1997): 10.2s Sonoran Desert, 13.1 upper Gila Mountains, 14.3 western Pacific coastal plain hills and canyons, 13.2 western Sierra Madre, 12.1 western Sierra Madre piedmont, and 10.4 Chihuahuan Desert. This delimitation follows Gutzler (2004): (right) 32-km resolution NARR grid points within the NAMS region.

Comrie 1997). But, while the land surface energy budget is known to play a crucial role in the development of the monsoon, many lingering questions remain regarding the effect of land surface water and energy fluxes in monsoon initiation and sustenance (Higgins et al. 2003; Higgins and Gochis 2007). Land surface memory provides some predictive potential in the monsoon regions. In much the same way as increased Eurasian snow cover leads to a decrease in monsoon rainfall over Southeast Asia (Barnett et al. 1989), positive (negative) soil moisture anomalies in the southwestern United States, generally related to winter snowfall anomalies, suppress (enhance) summer monsoon rainfall (Gutzler and Preston 1997; Small 2001). On the other hand, soil moisture anomalies located within the NAMS domain (Fig. 1) generate a positive feedback between soil moisture and summer precipitation (Small 2001), as positive anomalies potentially enhance rainfall by decreasing boundary layer height, increasing moist static energy, and increasing instability (Eltahir 1998; Betts et al. 1996). Vegetation clearly plays an important role in controlling surface moisture and energy fluxes to the atmosphere, as areas with abundant transpiration within the NAMS domain tend to have higher net radiation (Watts et al. 2007). The relationship is further complicated by topography, as the strength of land–atmosphere coupling is modulated by the elevation of the terrain, which also controls the ecosystem type (Vivoni et al. 2007).

While most studies have focused on the effect that soil moisture has on the overlying atmospheric energy budget, surface moisture in the NAMS region also directly contributes to precipitation by providing evaporative sources for precipitable water. Bosilovich et al. (2003) used a general circulation model (GCM) with water vapor tracers to identify the source regions for the NAMS precipitation. They found that during May, June, and July continental moisture sources from Mexico are the dominant source of water vapor for the western Mexico region (roughly corresponding to the NAMS region), contributing to approximately 30% of the total precipitation within the region. Their study also concludes that the wettest monsoons have the largest continental sources, while drier monsoons have less local sources of precipitation. In this work, we will quantify precipitation recycling using the Dynamic Recycling Model (DRM) developed by Dominguez et al. (2006) [see Dominguez and Kumar (2008, hereafter Part I) for a detailed explanation]. While the water vapor tracer analysis of Bosilovich et al. (2003) includes more detailed physics than the analytical model, our work uses the higher-resolution NARR assimilated data, which provides improved estimates of land–atmosphere variables compared to the GCM and is able to resolve the Gulf of California. Our work focuses primarily on the daily-to-intraseasonal time scale in order to better understand the physical mechanisms that drive recycling spatiotemporal variability at these time scales. Furthermore, we will perform a detailed analysis of the source and sink regions of recycled precipitation within the NAMS domain.

The goal of this work is to better understand the role

that precipitation recycling plays in the NAMS hydrometeorologic system. Some of the questions we would like to address are: How much of the total NAMS precipitation comes from evapotranspiration within the NAMS domain? Furthermore, as a link between the long-memory soil moisture storage and the atmosphere, what is the role of precipitation recycling in NAMS sustenance? Which are the primary source and sink regions for recycled precipitation? What is the spatial distribution of precipitation recycling? How are vegetated environments affected by recycling of moisture?

This is the second of a two-part study on precipitation recycling over North America. While the first part analyzed the central U.S. plains, a region of abundant soil moisture, here we focus on the arid and semiarid regions of southwestern United States and northwestern Mexico. As we have shown in Part I, in the central U.S. plains the dominant mechanism is a negative feedback that ensures, even when advected precipitation is low, the land continues to feed moisture into the overlying atmosphere and contribute to rainfall. The NAMS, on the contrary, shows a predominantly positive feedback where precipitation enhances evapotranspiration and subsequent precipitation of recycled origin. However, as we will show in this work, during long monsoons the NAMS region exhibits a similar negative feedback mechanism as for the central U.S. plains. During long monsoons, precipitation of recycled origin is significantly enhanced during periods of low advected moisture, thus bringing additional rainfall that creates favorable hydroclimatological conditions to the vegetated regions.

Section 2 gives a brief overview of data and methodology used in this work. The reader is referred to Part I for a more detailed description of the recycling model, the multivariate singular spectrum analysis (M-SSA) statistical technique, and the data. Section 3 focuses on the average hydroclimatology of the NAMS region and uses M-SSA to characterize the seasonal variability of different land–atmosphere hydrologic variables, including recycling. Section 4 further explores the variability within the monsoon system and the role that precipitation recycling plays in the sustenance of the NAMS. Our goal in this section is to unravel the physical mechanisms that drive precipitation recycling in the region through a detailed spatial and temporal variability analysis of the land–atmosphere variables. Summary and conclusions of the work are discussed in section 5.

2. Data and methodology

As in Part I, we use data from the North American Regional Reanalysis (NARR) (Mesinger et al. 2006) which was developed as an improvement upon the earlier National Centers for Environmental Prediction–National Center for Atmospheric Research (NCEP–NCAR) Global Reanalysis, and has focused significant effort on improved hydrologic modeling. Twenty-two years (1985–2006) of warm season (1 April–30 September) 3-hourly data was obtained from NARR, and daily values were later derived from this data. The NARR grid points corresponding to the NAMS region are depicted in Fig. 1. Because the assimilation process depends on the quality and quantity of observations, there is a sharp difference in the quality of the NARR data between Mexico and the United States. This can clearly be seen in the precipitation and evapotranspiration fields throughout this work. Furthermore, it is important to reiterate that NARR is an assimilated dataset and, without any climatological observations of evapotranspiration (ET), the estimates of ET in the dataset are subject to error (Nigam and Ruiz-Barradas 2006). Because we lack the data to calculate the error in NARR ET, we have estimated the uncertainty in the recycling ratio (RR) as a function of the ratio of "actual" ET over NARR-calculated ET (ETnarr) for average conditions over the NAMS region; the analysis is shown in Fig. 2. Using average NARR ET (ET/ETnarr = 1), precipitable water, and winds over the region we calculate a regional recycling ratio of around 15.6%. However, if the actual ET were 50% larger, RR would be 22.6%, while a 50% decrease in ET would give us 8.2% RR. Consequently, for the range of values in the NAMS, we have an approximate linear relationship between ET and NARR. It is important to point out that

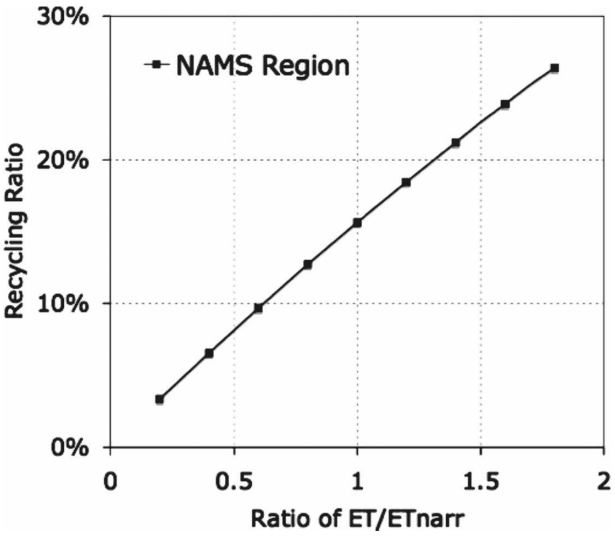

FIG. 2. Recycling ratio calculated using the DRM as a function of the ratio of "actual" ET over NARR calculated ET (ETnarr) for average conditions over the North American monsoon region.

the primary focus of this analysis is to understand the mechanisms that drive variability in precipitation recycling: if NARR ET has a consistent bias over the region, this will in no way affect the variability analysis we have performed. Unfortunately, at this point there is no way to analyze the effect that nonlinear ET errors will have on our RR calculations. For this reason we underscore that the precipitation recycling analysis reflects the hydrologic cycle as obtained with the dynamically consistent NARR data.

The geographical classification system used in this research is the Level II ecological regions of North America (CEC 1997). The NAMS region, as delineated by Gutzler (2004), is composed of six very distinct Level II ecoregions (see Fig. 1) described in CEC (1997). The driest ecoregions are the Sonoran and Chihuahuan Deserts where the predominant arid-region vegetation includes shrubs, grasses, and cacti. Originally, ecoregion 10.2 included both the Mojave and Sonoran Deserts but, since the Mojave Desert receives most of its rainfall during the winter months (Warner 2004), we excluded this area. At higher elevations (1100–2500 m) we find the semiarid western Sierra Madre piedmont, where blue grama short grass is dominant except for scrublands and forests in the transition zones leading to the western Sierra Madre and upper Gila Mountains. The high mountain ranges, with elevations up to 3000 m, have temperate climates ideal for evergreen or deciduous forests, with conifers and oaks. Cloud forests are common in the upper elevations. Descending from the mountains to the lower altitudes, we find the Pacific coastal plains hills and canyons. Seasonally dry tropical forest vegetation is abundant in the region where low deciduous and subdeciduous forests dominate. This seasonally dry tropical region receives intense rainfall during the summer months and experiences dramatic green-up (Higgins et al. 2003).

a. Precipitation recycling

Analytical models of precipitation recycling provide a simple and computationally efficient way of estimating the relative contribution of recycled and advected precipitation within a region. We use the DRM (Dominguez et al. 2006), which assumes that the atmosphere is fully mixed and hence does not account for incomplete vertical mixing. Using water vapor tracers, Bosilovich (2003) demonstrate that this assumption is not always valid and might affect recycling calculations in certain regions. To address this problem, Burde (2006) modifies traditional recycling models by including a parameter K, which accounts for "fast recycling" or precipitation originating from evapotranspiration that does not mix with advected moisture. The drawback is that the calculation of K requires some a priori knowledge of P_m/P and w_m/w (the ratios of recycled to total precipitation and precipitable water), which are characteristic of the region. This information is not easily obtained for the NAMS domain, and is probably highly variable in space owing to the complex topography of the region. Our results do not incorporate the K estimate and therefore assume that the atmosphere is fully mixed. Because it is likely that precipitation will be composed preferentially from moisture in the lower atmosphere, where recycled moisture dominates, the estimates using the DRM will have a bias toward lower recycling ratios.

b. Multichannel singular spectrum analysis

While in Part I (central U.S. plains) we used M-SSA primarily to extract oscillations in the hydroclimatological data with periodicities less than 40 days, in this particular application we are mainly concerned with extracting the seasonal variability in the data (noise reduction). The reason is that the oscillatory components in the NAMS domain were not robust to the change in window size, while the nonlinear trend modes (seasonal variability) were invariant whether we used a 60- or 40-day window. The advantage of using M-SSA, as opposed to other smoothing techniques, is that the nonlinear trends are generated from the lagged covariance matrix of *all variables* and, for this reason, it will extract variability common to the entire dynamic system containing these variables. Our results present the reconstructed components (RCs) using only the first few principal components, keeping in mind that the original time series can be obtained as the sum of all the RCs. The sum of a few reconstructed components will contain a percentage of the variability in the original data: a larger percentage indicates a better representation of the original time series.

3. North American monsoon

a. Climatology

The NAMS transforms the regional atmospheric and surface hydrology, and consequently the signature of the monsoon can be seen in many different hydrologic variables. In Fig. 3, we can see the normalized (1985–2006) daily precipitation, recycling ratio, evapotranspiration, and sensible heat (SH) and their variability throughout the warm season. The normalized variables are obtained by averaging over the entire NAMS region and 22-yr period, then subtracting the seasonal mean and dividing by the standard deviation. It is clear

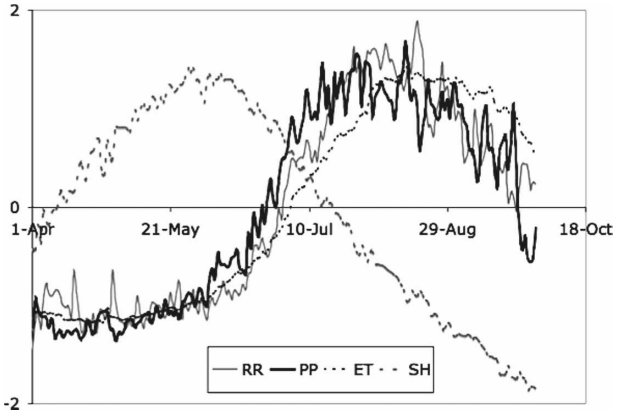

FIG. 3. Warm season daily precipitation (PP), recycling ratio (RR), evapotranspiration (ET), and sensible heat (SH) averaged over the entire NAMS region and over the 22-yr period (1985–2006), then normalized by subtracting the seasonal mean and dividing by the standard deviation.

TABLE 1. Surface and atmospheric variables used to characterize the NAMS. The variables derived from NARR are described in detail in Part I.

Variable	Notation	Source
Precipitation	PP	NARR
Convective precipitation	PC	NARR
Precipitable water	PW	NARR
Boundary layer height	HC	NARR
Zonal moisture flux	QU	Derived NARR
Meridional moisture flux	QV	Derived NARR
Moisture flux divergence	DV	Derived NARR
u	Uw	Derived NARR
v	Vv	Derived NARR
Wind	WW	NARR
Potential evapotranspiration	PE	NARR
Evapotranspiration	ET	NARR
Sensible heat	SH	NARR
Surface air temperature	TM	NARR
Soil moisture (0–200 cm)	SM	NARR
Recycling ratio	RR	Derived NARR

from this figure that with the monsoon rains comes an increase in recycling ratio as well as significant changes in the surface energy fluxes.

What is the role that recycling plays within the NAMS hydroclimatology? As a first step to answer this question, we perform M-SSA for the set of 16 variables listed in Table 1, averaged in space over the entire monsoon region and averaged in time over the 22 years of analysis, thus generating mean warm season (April–September) time series. This will give us an idea of the characteristic NAMS signature for the set of hydroclimatologic variables, including the recycling ratio. M-SSA analysis using a window of 60 days yields 960 modes (16 variables times 60-day window length). Of these modes, only the first five account for 88% of the total variability in the data. Figures 4 and 5 show the sum of the first five reconstructed components for all 18 variables (precipitation is plotted in every panel as a dash–dot line). The bold line presents the sum of the first five modes for the given variable, while the thin line shows the original normalized data (which is equal to the sum of all the reconstructed components). The percent of variance of the original time series captured by the first five modes is shown to give an indication of how close our smoothed data is to the original time series.

Figures 4 and 5 show that the first five modes capture, not only the sharp increase in precipitable water (PW) and precipitation (PP), including convective precipitation (PC), but in most cases rapid changes related to other variables in the monsoon system. For example, the monsoon leads to an increase in soil moisture (SM), ET, and RR and a decrease in SH, wind magnitude (WW), and cloud-base height (HC). These results indicate that the monsoon system changes the surface conditions and enhances convective potential of the atmosphere (Small 2001). The increase in SM, ET, and RR lag the onset of monsoon precipitation (as seen in Fig. 4); this indicates that precipitation originating from local ET does not have much impact on the onset of monsoon precipitation but rather on the sustenance of rainfall in the NAMS.

Because the boundary layer height over land is primarily thermally generated, it is strongly linked to the sensible heat flux (Betts et al. 1996). As precipitation increases in the NAMS region, soil moisture increases and evapotranspiration increases, providing moisture to the overlying atmosphere. At the same time, the sensible heat flux decreases and there is a marked reduction in cloud base height. The low boundary layer height, in addition to the increased moisture in the air from advective and recycled origin, increases moist static energy (following the mechanism hypothesized by Eltahir 1998), creating a favorable environment for convective storms.

The characteristic reversal in atmospheric circulation can clearly be seen in the zonal wind (Uw) and zonal moisture flux (QU). The solid horizontal line in the Uw and QU panels of Figs. 4 and 5 denote the change from westerly to easterly flow. It has been shown that, over the Sonoran Desert and in central Arizona and New Mexico, air temperature at the surface (TM) peaks just prior to the onset of the monsoon (Xu et al. 2004); this is clearly seen in Fig. 4. The TM increase causes an increase in saturation vapor pressure and, consequently, in potential evapotranspiration (PE). Both TM and PE decrease as the monsoon rains begin. As ex-

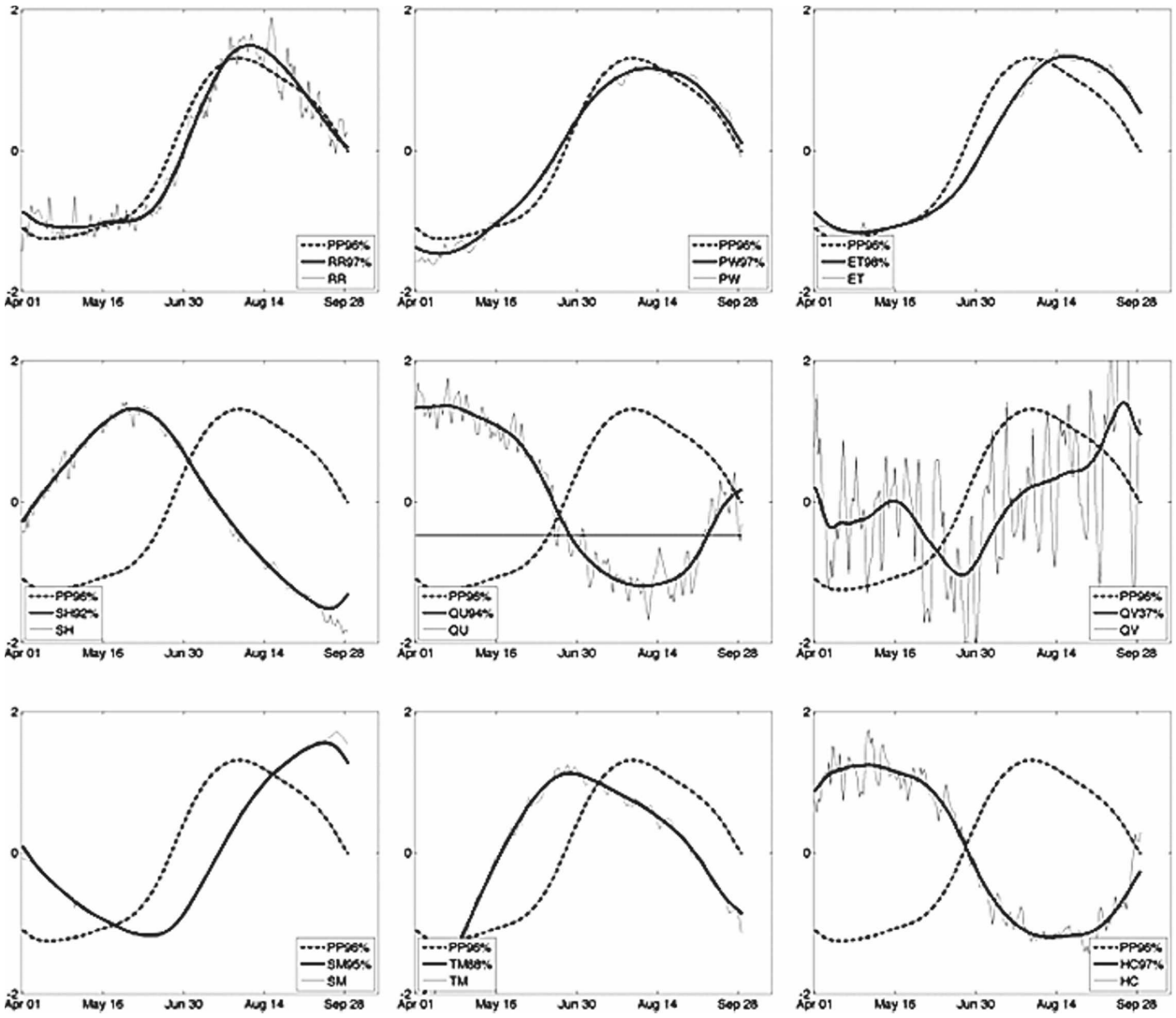

FIG. 4. Sum of the five dominant reconstructed components obtained using M-SSA for the 18 variables listed in Table 1 (bold line), overlaid by the original normalized time series (thin line). The analysis is done for the average daily 1985–1995 data over the entire NAMS region. The sum of the five reconstructed components of precipitation is plotted as the bold dash–dot line in every panel to indicate the start of the monsoon season. The label indicates the percent of the variability in the original time series captured by the reconstructed modes.

pected, the increased precipitation generates a lagged response in the soil moisture. Because the NARR SM is calculated as the water content in the top 2 m of soil, the high-frequency variability in surface soil moisture is dampened by averaging over the lower layers. For this reason the soil moisture time series is smooth compared to other variables in the dataset.

The analysis shows that the five dominant modes of meridional moisture flux (QV) capture only 37% of the variability in the data and do not show an abrupt change as the monsoon commences. It has been generally understood that the moisture surges entering the region from the Gulf of California significantly contribute to monsoonal precipitation (Stensrud et al. 1995) but, because the moisture flux has been averaged over the entire region (see Fig. 1), we do not capture the important meridional component. If the analysis is repeated with QV averaged over the Sonoran Desert (region 10.2s), we obtain a much stronger meridional moisture flux signal, as seen in Fig. 6.

The results from Figs. 4 and 5 show that, on average, precipitation recycling forms part of a positive land–atmosphere feedback mechanism. The recycling ratio peaks during mid-August at the height of the monsoon season. The intense monsoonal precipitation brings an increase in soil moisture and evapotranspiration

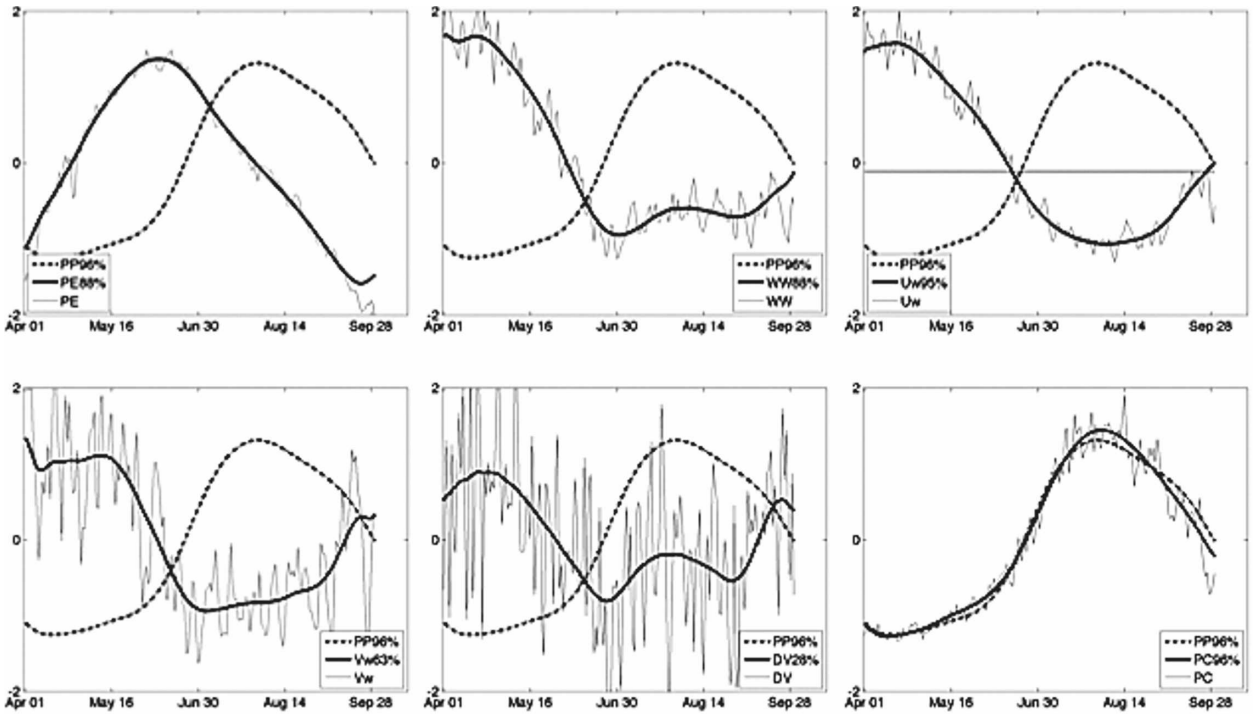

FIG. 5. As in Fig 4 but for the variables indicated in the panel legends.

throughout the season. The additional water originating from evapotranspiration will provide moisture to the overlying atmosphere and contribute to monsoon rainfall as precipitation of recycled origin.

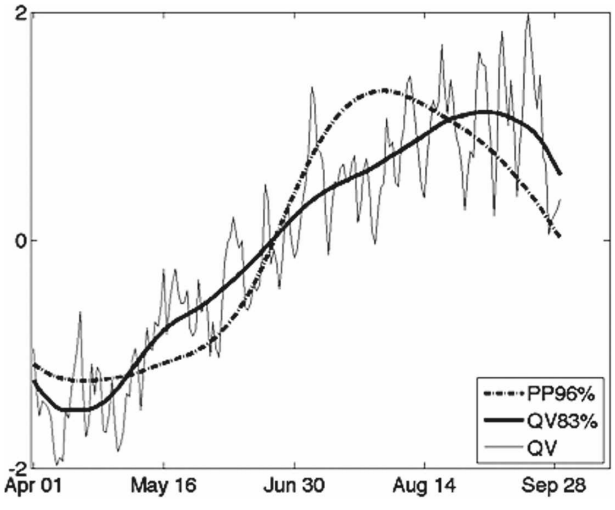

FIG. 6. Sum of the five dominant reconstructed components obtained using M-SSA (bold line), overlaid by the original normalized time series (thin line) of warm season meridional moisture flux over the Sonoran Desert obtained using M-SSA. The sum of the five reconstructed components of precipitation is plotted as a bold dash–dot line to indicate the start of the monsoon season.

b. *Interannual variability*

Until now, we have focused on the average characteristics of the North American monsoon, but its interannual variability has important ecological as well as socioeconomic consequences for the region. Several studies have focused on quantifying the total amount of warm season precipitation as a measure of the strength of the monsoon (Gutzler 2004; Higgins and Mo 1998). Additionally, we need to define a measure of monsoon duration. To do this, we first calculate the total precipi-

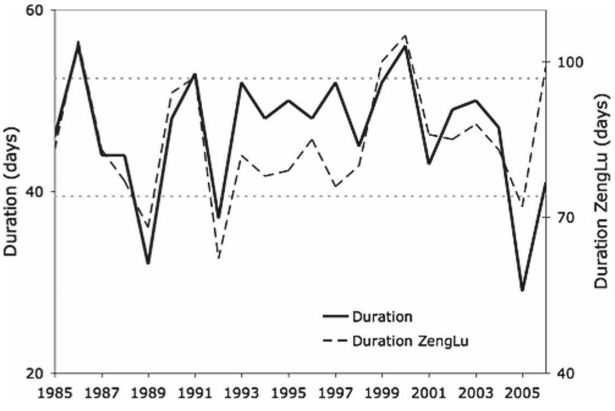

FIG. 7. Monsoon duration calculated using precipitation quartiles (solid line) and using the methodology of Zeng and Lu (2004) (dashed line) for the years 1985–2006.

TABLE 2. Date and total accumulated rainfall corresponding to stage 1, stage 2, and stage 3 for each year. Each stage corresponds to one quarter, one half, and three quarters of the total rainfall from 1 Jun to 30 Sep. The last two columns summarize the total rainfall and the total duration (days between stages 1 and 3) of the monsoon.

	Stage 1		Stage 2		Stage 3		Total	
Year	Date	Rain (mm)	Date	Rain (mm)	Date	Rain (mm)	Rain (mm)	Duration (days)
1985	13 Jul	71.73	30 Jul	143.45	28 Aug	215.18	286.9	46
1986	2 Jul	82.39	29 Jul	164.79	27 Aug	247.18	329.57	56
1987	15 Jul	70.08	4 Aug	140.17	28 Aug	210.25	280.34	44
1988	7 Jul	79.65	30 Jul	159.29	20 Aug	238.94	318.58	44
1989	22 Jul	70.6	7 Aug	141.21	23 Aug	211.81	282.42	32
1990	14 Jul	102.89	4 Aug	205.78	31 Aug	308.67	411.56	48
1991	11 Jul	69.15	3 Aug	138.3	2 Sep	207.46	276.61	53
1992	20 Jul	47.56	7 Aug	95.11	26 Aug	142.67	190.23	37
1993	9 Jul	75.83	31 Jul	151.67	30 Aug	227.5	303.33	52
1994	13 Jul	39.06	8 Aug	78.11	30 Aug	117.17	156.23	48
1995	15 Jul	53.19	13 Aug	106.38	3 Sep	159.58	212.77	50
1996	12 Jul	59.38	11 Aug	118.76	29 Aug	178.14	237.52	48
1997	9 Jul	48.58	5 Aug	97.16	30 Aug	145.74	194.32	52
1998	16 Jul	55.24	7 Aug	110.48	30 Aug	165.72	220.97	45
1999	4 Jul	46.95	25 Jul	93.89	25 Aug	140.84	187.78	52
2000	25 Jun	42.17	20 Jul	84.35	20 Aug	126.52	168.69	56
2001	16 Jul	53.03	4 Aug	106.05	28 Aug	159.08	212.11	43
2002	15 Jul	56.04	2 Aug	112.09	2 Sep	168.13	224.18	49
2003	16 Jul	67.48	12 Aug	134.96	4 Sep	202.45	269.93	50
2004	16 Jul	75.61	5 Aug	151.22	1 Sep	226.83	302.44	47
2005	23 Jul	47.92	6 Aug	95.84	21 Aug	143.76	191.67	29
2006	18 Jul	69.87	4 Aug	139.74	28 Aug	209.61	279.48	41

tation that falls over the region for the period between 1 June and 30 September for each year. We then estimate the date when one quarter, one half, and three quarters of the total rainfall occurred (stage 1, stage 2, and stage 3, respectively). The number of days between stage 1 and stage 3 (interquartile range) gives a measure of length of the monsoon. This calculation of monsoon length is not a measure of monsoon onset or demise, like other methods such as that of Zeng and Lu (2004), but is solely based on the temporal distribution of monsoonal precipitation in time. Figure 7 presents the interannual variability of monsoon duration using both the proposed precipitation quartile method and the methodology of Zeng and Lu (2004) and shows that the two methodologies are significantly correlated (0.67). Table 2 lists the date and total rainfall for each of the three stages calculated using precipitation quartilesand gives the total rainfall and total duration of the monsoon for each of the 22 years.

Monsoons of long duration are especially interesting when studying land–atmosphere interactions because soil moisture provides a source of memory for the hydroclimatologic system (Koster et al. 2004). Consequently, the land surface, through its impact on moisture and energy fluxes, could play an important role in monsoon maintenance. Precipitation recycling is one of the key mechanisms that links the slow varying surface processes and the overlying atmosphere. For this reason, it is important to understand the role that precipitation recycling plays in monsoon variability, with special emphasis on long monsoons.

4. Recycling and the monsoon

Precipitation recycling variability in the monsoon region is inextricably linked to precipitation and evapotranspiration variability. While rainfall provides moisture for precipitation that can later be evaporated, it also increases atmospheric humidity. As low-level humidity increases, the vertical gradient of specific humid-

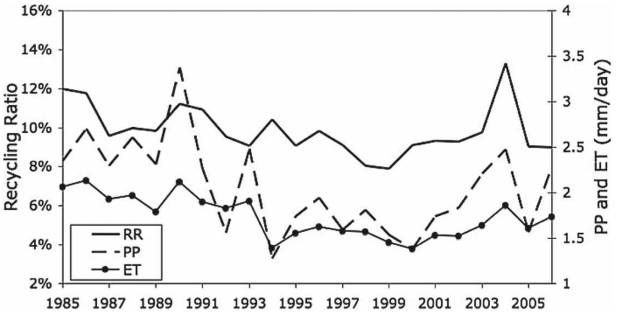

FIG. 8. Average daily RR (solid line), PP (dashed line), and ET (circle marker) from 1 Jun to 30 Sep for the years 1985–95.

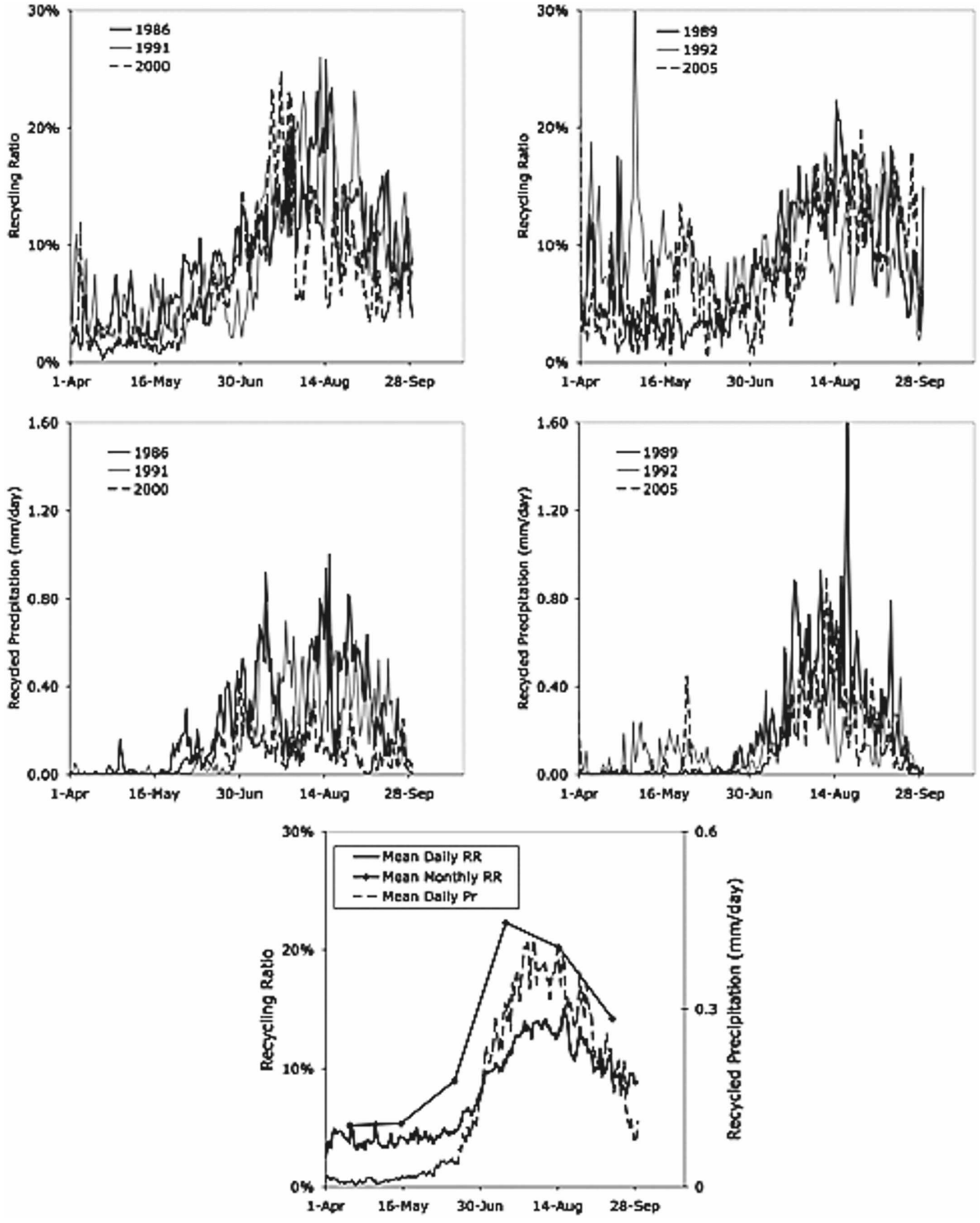

FIG. 9. (top), (middle) RR and recycled precipitation of recycled origin for the years 1986, 1991, and 2000 corresponding to the years of longest monsoons and 1989, 1992, and 2005 corresponding to the shortest. (bottom) The average (1985–2006) daily RR, monthly RR, and recycled precipitation.

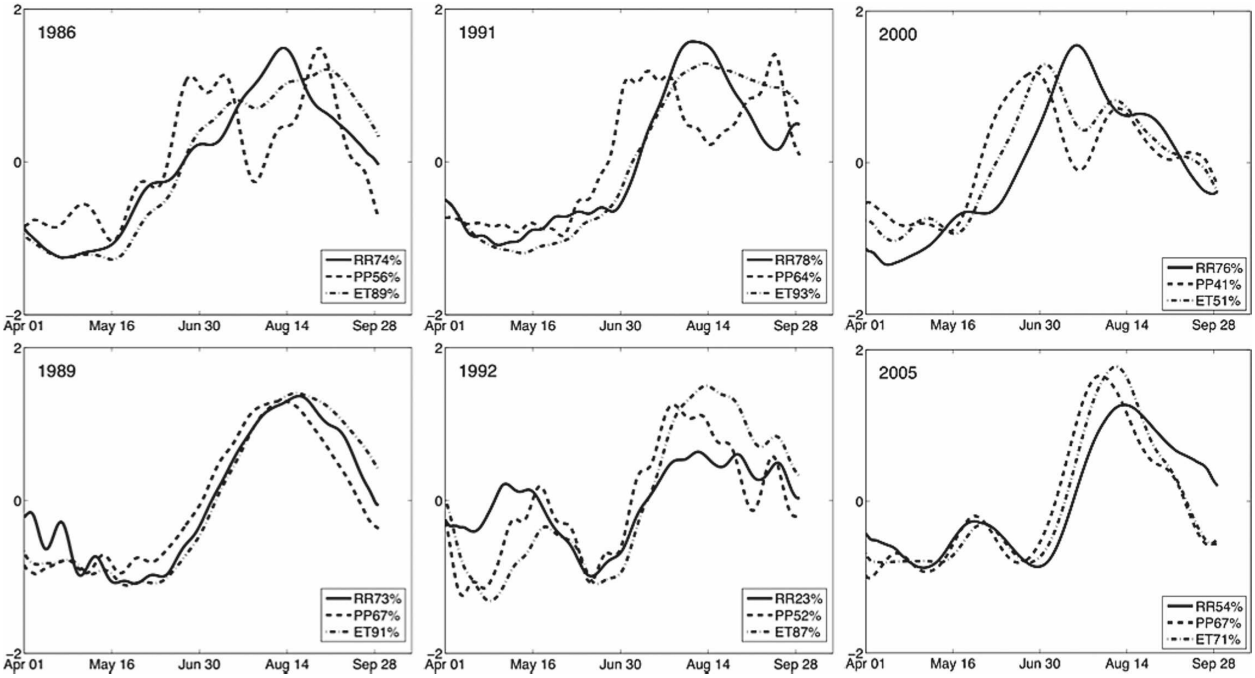

FIG. 10. Five dominant reconstructed modes of the 16-variable M-SSA analysis of PP (dashed), RR (solid), and ET (dash–dot) for five years: 1986, 1991, and 1993 corresponding to the years of longest monsoons, while 1989 and 1992 correspond to the shortest. M-SSA analysis is performed on the normalized data by subtracting the seasonal mean and dividing by the standard deviation.

ity decreases, bringing a proportional drop in evapotranspiration. Consequently, precipitation brings competing mechanisms that affect the variability of precipitation recycling: therefore, the important question is what mechanisms dominate? Figure 8 shows the average daily summer season (1 June–30 September) recycling ratio, precipitation, and evapotranspiration from 1985 to 2006. There is a statistically significant positive correlation between the recycling ratio with both precipitation (0.56 correlation coefficient) and evapotranspiration (0.63 correlation coefficient): both correlations are above the 95% threshold.

Looking back at Fig. 7, we see that the duration of the monsoon varies considerably from year to year. The summers with longest monsoons (above one standard deviation) are 1986, 1991, and 2000, while 1989, 1992, and 2005 present the shortest monsoons. Figure 9 presents the daily recycling ratio and precipitation of recycled origin for these six selected years and for the average of the 22-yr period. Precipitation of recycled origin is defined as the recycling ratio multiplied by the daily precipitation. As shown in the previous analysis, the recycling ratio and the precipitation of recycled origin are significantly enhanced as the monsoon enters the region. In agreement with the analysis of Bosilovich et al. (2003), the climatological recycling ratio shows a sharp increase in continental sources of moisture as the warm season progresses and then a slow decrease toward the end of the season. Our results are consistently about 10% smaller than in Bosilovich et al. (2003, see their Fig. 8a). This is mainly due to the larger region that they are considering; the lower resolution of the GCM analysis, which does not resolve the Gulf of California; and the assumption of a well-mixed atmosphere in the dynamical recycling model. The main inconsistencies between both studies are the months of May and June when we predict much smaller recycling ratios than in Bosilovich et al. (2003); the reason for this difference might be the larger continental region that they considered. The bottom panel of Fig. 9 also presents the average monthly recycling ratio for the region. Interestingly, the calculation of the recycling ratio using monthly average values of winds, humidity, and precipitation yields higher recycling ratios than the daily analysis. As shown in Part I, the recycling ratio is inversely proportional to wind velocity: because the monthly average dampens the wind variability in this region, the recycling ratios will be over estimated. Owing to the recycling ratio dependence on the highly variable wind velocities, a more realistic monthly recycling ratio will be obtained by averaging the daily recycling ratio values, as opposed to calculating the value of r using average monthly fields.

The summers of 1986, 1989, 1991, 2000, and 2005

show a pronounced increase in recycling in early July. For these years, the recycling ratios during the monsoon are consistently above 15% and can be as high as 25%. On the other hand, 1992 presents significant recycling ratios in the spring (late April, early May). In fact, it has the highest spring recycling of the 22-yr period, while recycling during the monsoon season is not as high as for other years.

As in the previous climatological analysis, we now perform M-SSA on each of the three years with longest monsoons and the three years with shortest monsoons. An interesting pattern is revealed by the analysis (Fig. 10). The summers of 1986, 1991, and 2000 present a characteristic pattern of rainfall and recycling comprising a precipitation peak at the beginning of the season and then a second precipitation peak toward the end of the season. Evapotranspiration continues to be high during the midsummer dry period, and we see a peak in the recycling ratio during mid-August. The selected years of short monsoon duration do not present this precipitation–evapotranspiration–recycling pattern. The bimodal distribution of summer rainfall is characteristic of the central and southern part of Mexico and most of Central America (Magaña et al. 1999), where the local name for the midsummer drought period is "canicula" or "veranillo" (which means the small dry season in Spanish). Douglas and Englehart (1996) also identified the characteristic double peak in summer precipitation using observed daily rainfall data in the Mexican state of Oaxaca. Our analysis shows that during monsoons of long duration this pattern migrates northward and can be seen throughout the NAMS domain. Furthermore, our results show that during long monsoons recycling ratios are enhanced during the drier midsummer period between precipitation peaks.

Because the actual amount of recycled precipitation is obtained by multiplying the recycling ratio by the total precipitation, the actual amount of recycled rainfall during the dry intermediate period is low. The importance of this intermediate period is that evapotranspiration from the soil and vegetation continues to provide moisture for precipitation even though the large-scale advective sources have dramatically decreased. While in the previous section we have shown that, on average, there is a positive feedback between soil moisture/evapotranspiration and precipitation (see Fig. 4 and discussion in section 3), the years of monsoon with longest duration show a different picture. They have an intermediate period of negative feedbacks; that is, reduced total precipitation promotes precipitation of recycled origin. To further explore this point, we examine other land–atmosphere variables and how they progress in relation to precipitation and recycling ratio during the 1986 long monsoon (Fig. 11). The first precipitation peak in 1986 is preceded by a temperature peak. In the midsummer drought period, we see a decrease in soil moisture with an increase in sensible heat and increased cloud base height. However, evapotrans-

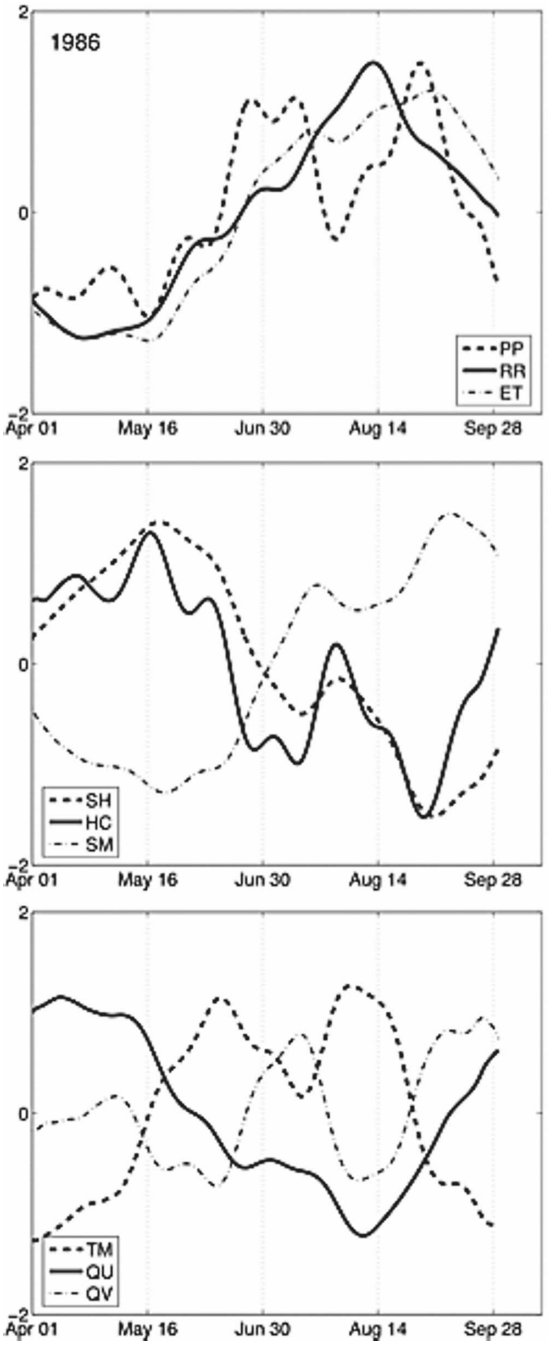

FIG. 11. Five dominant modes for the April–September 1986 daily data of RR, PP, and ET in addition to sensible heat (SH), cloud base height (HC), soil moisture (SM) and temperature (TM), and zonal (QU) and meridional (QV) moisture flux.

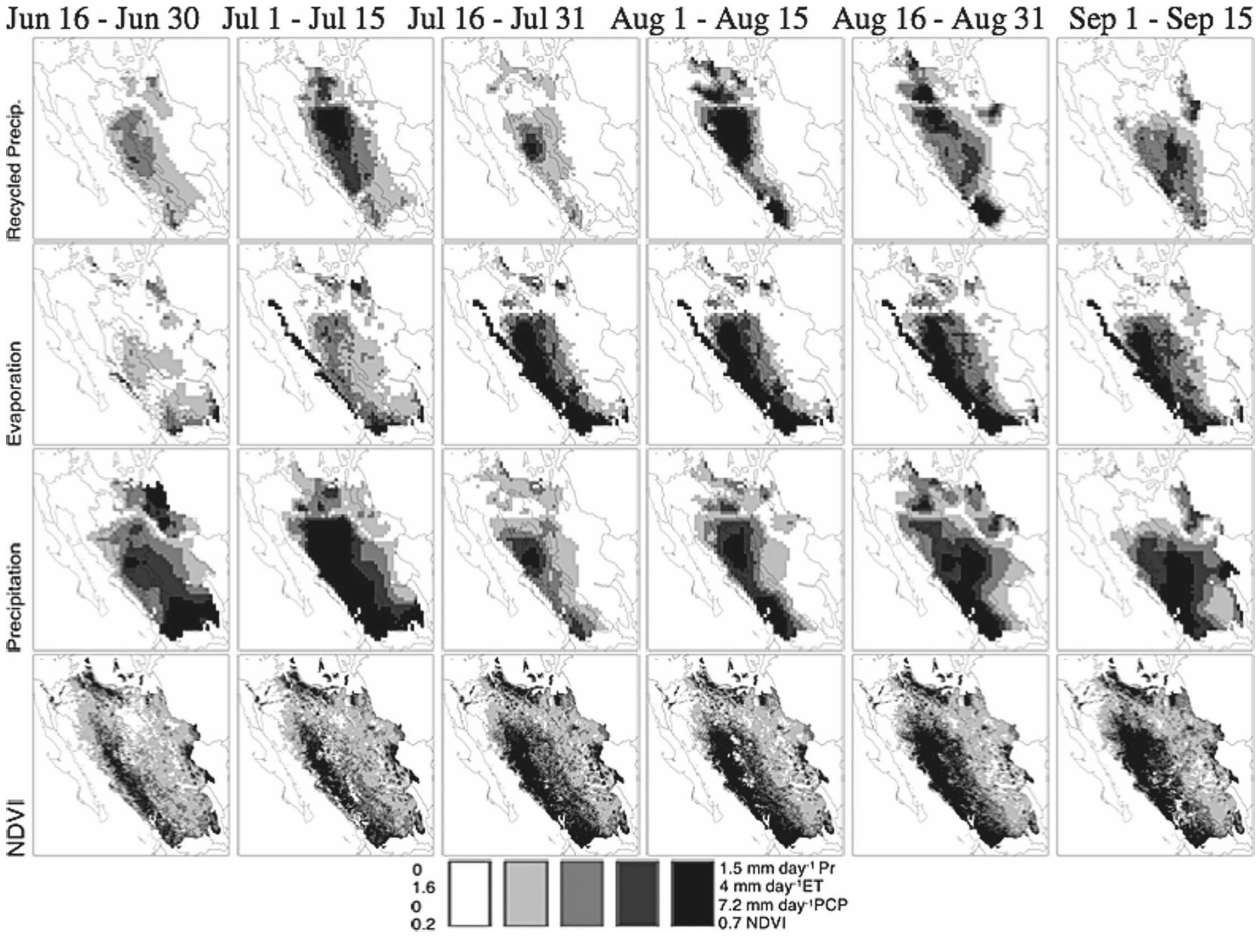

FIG. 12. Biweekly average daily precipitation of recycled origin, ET, PP, and NDVI during the warm season of 1986 (long monsoon): (from left to right) the end of June to the beginning of September.

piration slowly keeps increasing and continuously feeding into the overlying atmosphere: by mid-August the recycling ratio reaches its highest value. We can see that the peak in recycling coincides with the highest negative zonal flux anomaly, indicating that the air is mostly coming from the east. The second precipitation peak, of predominantly advective origin, comes at the end of the season during late August.

a. Spatial variability

To gain an understanding of the spatial distribution of the variables that modulate the recycling–precipitation signature, we again focus our attention on the year 1986, a long monsoon, and contrast it with 1989, a year of short duration. Figures 12 and 13 show the biweekly average of daily local recycling ratio, evaporation, precipitation and the normalized difference vegetation index (NDVI) for the warm seasons of 1986 and 1989, respectively. The NDVI data was obtained from the NOAA/NASA Pathfinder Advanced Very High Resolution Radiometer (AVHRR) 8-km data (Tucker et al. 2005) and is used here to compare the vegetation distribution with the evapotranspiration data as well as to corroborate the NARR output with a purely observational data source.

The NDVI data clearly shows that the most abundant vegetation is concentrated in the temperate western Sierra Madre and tropical Pacific coastal plains. As expected, this is also the region with the highest precipitation and evapotranspiration values of the NAMS domain. Interestingly, Figs. 12 and 13 show that, even though the recycled precipitation has a similar spatial distribution as the precipitation (because it is calculated as the local recycling ratio ρ times the precipitation), there is evidence of relocation of water as there is higher recycled precipitation to the northeast. The evapotranspired moisture in the southwest is transported north and east, causing the recycled precipitation to peak primarily in the northern Sierra Madre

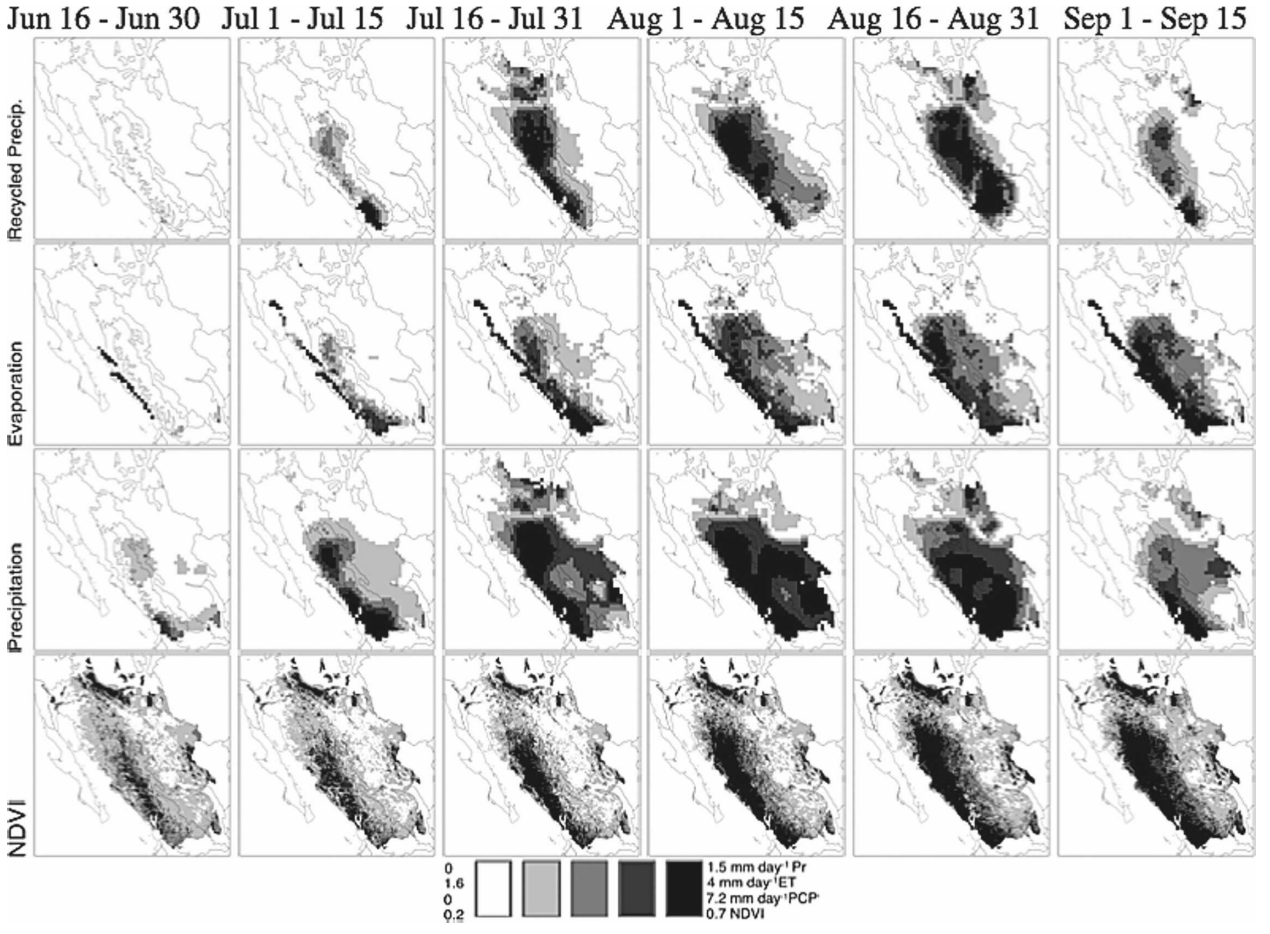

FIG. 13. As in Fig. 12 but for the warm season of 1989 (short monsoon).

Occidental and its piedmont. During both years we see high values of recycled precipitation in a large region that extends from the Sierra Madre Occidental all the way north to the upper Gila Mountains. The early July precipitation peak in 1986 (Fig. 12) is followed by intense evapotranspiration that remains high throughout the season. Figure 13 clearly shows that 1989 did not have the double peak in precipitation characteristic of long monsoons, and the evapotranspiration closely follows precipitation.

To complement Fig. 12 and get a better understanding of the dynamics during long monsoons, in Fig. 14 we present ecoregion-average values of local RR, recycled precipitation (Pr), ET, PP, and NDVI during 1986 (see also Fig. 1 for ecoregion boundaries). The recycled precipitation for each ecoregion is calculated as the precipitation falling within the ecoregion originating as evapotranspiration from NAMS region; by dividing the recycled precipitation by the total precipitation falling in the ecoregion we can obtain the local recycling ratio. One of the most interesting features of Fig. 14 is that ecoregions 12.1, 13.2, and 14.3 maintain a high level of evapotranspiration and vegetation greenness during the dry period of 1986. This translates into a high recycling ratio, even though the actual precipitation of recycled origin decreased (because total precipitation decreased). Even though advected precipitation decreased during the 1986 midsummer drought, evapotranspiration and recycling were still active, creating a feedback that helped maintain vegetation health. If the vegetation and evapotranspiration remained active during the dry period of 1986 but the total soil moisture decreased during this same period (as seen in Fig. 11), we can conclude that transpiration was the main contributor to ET. This highlights the importance of vegetation in providing moisture for recycled precipitation. This analysis also shows the important spatial and temporal similarities between NDVI and ET, providing confidence about the NARR-derived evapotranspiration.

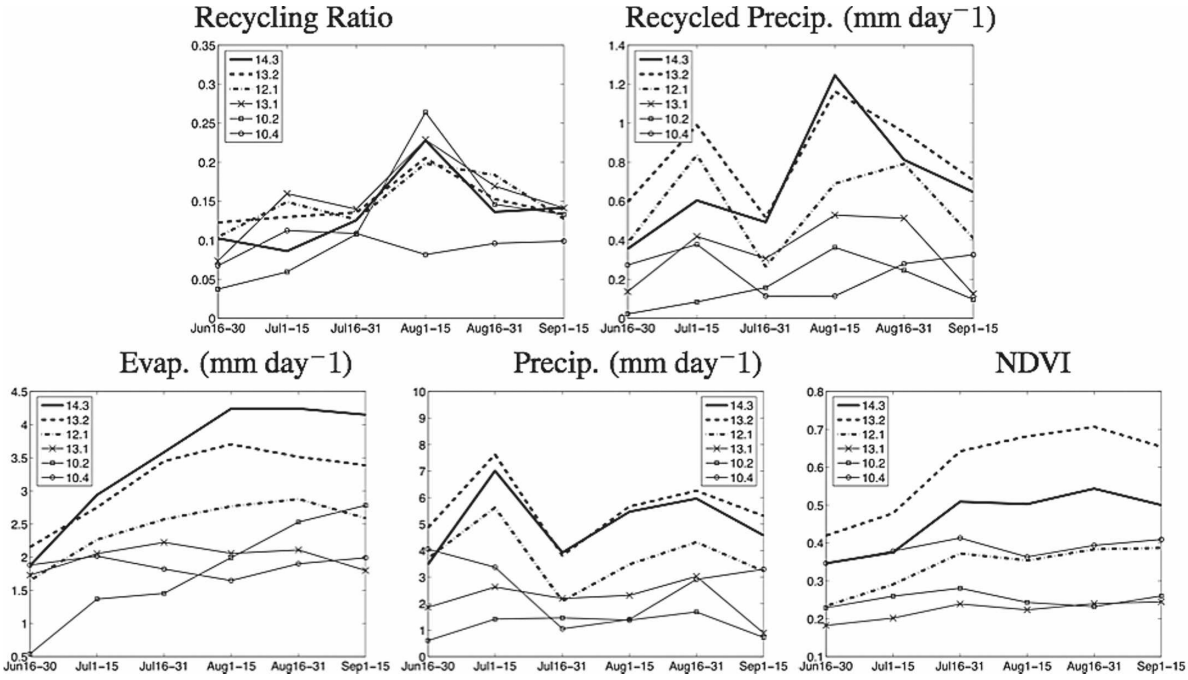

FIG. 14. Level II ecoregion-average RR (fraction of total precipitation originating as ET from NAMS region), ET, PP, and NDVI for 1986. The ecoregions are 13.1 upper Gila Mountains, 10.2 Sonoran Desert, 12.1 western Sierra Madre piedmont, 10.4 Chihuahuan Desert, 14.3 western Pacific coastal plain hills and canyons, and 13.2 western Sierra Madre. The *x* axis corresponds to the 15-day periods (left to right) beginning (16–30 Jun) and (far right) ending (1–15 Sep).

b. Moisture paths

When performing the recycling ratio calculation using the formulation of Dominguez et al. (2006), we are effectively following the atmospheric moisture along the paths defined by the u and v velocities (where u and v are, respectively, the zonal and meridional moisture flux divided by the total precipitable water, as shown in Part I). Throughout the trajectory, we calculate the ratio of moisture from evaporative origin (ε) to precipitable water in the column (ω), and integrate it from the time the moist air enters the region until the water precipitates (time τ). The local recycling ratio (R) at each grid point is a function of the integrated ratio:

$$R(\chi, \xi, \tau) = 1 - \exp\left[-\int_0^{\tau} \frac{\varepsilon(\chi, \xi, \tau)}{\omega(\chi, \xi, \tau)} \partial\tau' \right]. \quad (1)$$

The paths defined by the u and v velocities are particularly interesting as they represent the moisture-weighted trajectory of the air. The value of ε/ω along the path will indicate the regions along this trajectory that significantly contribute to the local recycling ratio; these will be the dominant source regions of evaporative moisture.

Figure 15 presents a detailed analysis for 10 August 1986. This day was selected because it presents one of the highest recycling ratios of 1986, and the paths are less dense than for 15 August (the day with highest recycling ratios), making it easier to visualize the paths. Although we cannot make generalizations from only one day of the analysis period, Fig. 15 clearly shows that the spatial variability of evapotranspiration translates into different ε/ω ratios throughout the paths. In Fig. 15c we have selected three paths and denoted the ratio ε/ω for each grid point in the path as a shaded bar. The darkest shading denotes the regions that make the largest contribution of evapotranspired moisture. For these three paths, the air enters the region through the east, where there is little contribution of ET as the air crosses the Chihuahuan Desert: however, as the air traverses the Sierra Madre Occidental and the western Pacific coastal plains we see how evapotranspiration from these areas significantly contributes to the moisture content in the atmospheric column.

5. Conclusions

The North American monsoon system abruptly transforms the hydrology of the North American southwest. In this work, we take a set of 16 land–atmosphere variables to represent the hydroclimatology of the monsoon and use M-SSA to extract nonlinear trends in the

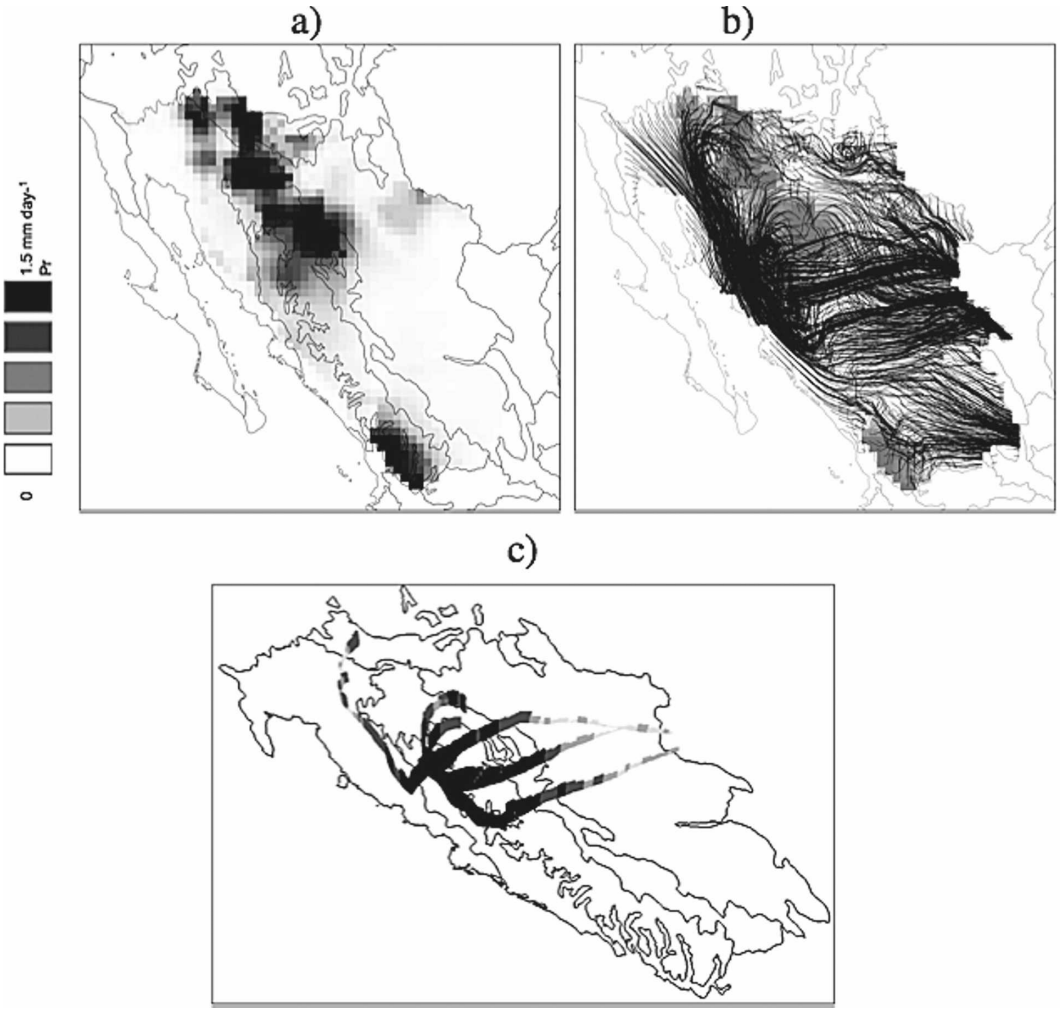

FIG. 15. The 10 Aug 1986 (a) local RR; (b) atmospheric paths of moisture at every grid point used to calculate the local RR; (c) three selected paths where the ratio of ET to precipitable water (ε/ω) is represented as shaded bars, the darker bars indicate a larger contribution to evapotranspired moisture (the wind direction is generally from east to northwest).

data while at the same time selecting only the variability common to all of the variables. Our study uses the North American Regional Reanalysis (NARR) data throughout the analysis and, while this is currently the best available dataset for extended spatiotemporal analysis over North America, it is important to keep in mind that this is an assimilated dataset and hence is only as good as the underlying model and observations. The most uncertain variable in our analysis is evapotranspiration; consequently, any consistent bias in ET will translate into changes in the recycling calculations.

Our main focus is to understand precipitation recycling as part of the dynamic NAMS system. The first five M-SSA modes of average 1985–2006 daily data capture many of the characteristics of the monsoon that have been widely discussed in the literature, such as the abrupt increase in precipitation and precipitable water, the temperature peak prior to the rains, the shift from westerly to easterly winds and consequent shift in zonal moisture flux, and the increase in northerly moisture flux confined to the Gulf of California coastal region. Furthermore, we see an increase in evapotranspiration and recycling ratio and a decrease is sensible heat and the cloud base height.

The climatological analysis of NAMS precipitation recycling reveals a positive feedback mechanism between monsoon precipitation and subsequent increase in precipitation of recycled origin. The study by Koster et al. (2004) has shown that there is a large region extending from the U.S. Great Plains down to northern Mexico where there is a strong impact of soil moisture on precipitation. Our analysis over the NAMS region,

which is embedded within the region delineated by Koster et al. (2004), shows that precipitation recycling is one of the mechanisms responsible for this positive feedback. In agreement with previous work, our study finds that evapotranspiration within the NAMS region significantly contributes to monsoon rainfall after NAMS onset. Recycling ratios during the monsoon are consistently above 15% and can be as high as 25%. While monsoon rainfall and evapotranspiration are predominantly located in the southwestern part of the domain, recycling is enhanced northeast of this region, indicating a relocation of soil moisture farther inland to drier regions in the north.

Focusing our analysis on the three years with longest monsoons in the 1985–2006 period, an interesting asynchronous pattern between precipitation and recycling ratio is revealed. The longest monsoons present a characteristic double peak in precipitation. Intense rainfall during late June and early July is followed by a period of dry conditions and a subsequent peak in late August precipitation. Contrary to what one might expect, recycling peaks during the intermediate dry period. Further inspection of other land–atmosphere variables during a long monsoon reveals that the period of decreased precipitation is accompanied by changes in many other land–atmospheric conditions that lead to the recycling peak. Our results present one of the feedback mechanisms modulating precipitation during monsoons of long duration. After the first precipitation pulse, atmospheric conditions are drier and evapotranspiration is enhanced during mid-August. The moisture of evaporative origin, originating predominantly in tropical forests in the southwest part of the domain, is then transported north and east where it later falls as precipitation, contributing to as much as 25% of the total precipitation in the NAMS domain. Using NDVI data, we argue that precipitation of recycled origin brings moisture to regions that would otherwise be dry and, hence, helps maintain vegetation greenness during the midsummer dry period. In this sense, precipitation recycling is a mechanism for ecoclimatological stability in the NAMS region.

As the seasonally dry tropical forests of Mexico continue to be severely degraded by human activities—particularly agriculture, cattle ranching, and timber extraction—the region faces imminent changes to existing vegetation cover and evapotranspiration regimes. According to Masera et al. (1997), the mid-1980s was a period of intense vegetation perturbation with deforestation of around 668 000 ha, 75% of which was concentrated in tropical forests. This led to a deforestation rate of 1.9% yr^{-1} for deciduous tropical forests and 2.0% yr^{-1} in evergreen tropical forests. Trejo and Dirzo (2000) found an annual deforestation rate of seasonally dry tropical forest in the state of Morelos, Mexico, of 1.4% yr^{-1}. What effect does land cover change in Mexico have on evapotranspiration and subsequent precipitation of recycled origin? We believe this is an intriguing question for future studies aimed at understanding the effect of land cover change on NAMS hydroclimatology.

Acknowledgments. Support for this project has been provided in part by the National Science Foundation (NSF) Grant EAR 02-08009. The work is also supported by the National Aeronautics and Space Administration (NASA) under Award No. ESSF/O3-0000-0215. Any opinions, findings, and conclusions or recommendations expressed in this publication are those of the authors and do not necessarily reflect the views of NSF or NASA.

REFERENCES

Adams, D. K., and A. K. Comrie, 1997: The North American monsoon. *Bull. Amer. Meteor. Soc.,* **78,** 2197–2213.

Barnett, T. P., L. Dumenil, U. Schlese, E. Roeckner, and M. Latif, 1989: The effect of Eurasian snow cover of regional and global climate variations. *J. Atmos. Sci.,* **46,** 661–685.

Betts, A. K., J. H. Ball, A. C. M. Beljaars, M. J. Miller, and P. A. Viterbo, 1996: The land surface–atmosphere interaction: A review based on observational and global modeling perspectives. *J. Geophys. Res.,* **101,** 7209–7225.

Bosilovich, M. G., 2003: On the vertical distribution of local and remote sources of water for precipitation. *Meteor. Atmos. Phys.,* **80,** 31–41.

——, Y. C. Sud, S. D. Schubert, and G. K. Walker, 2003: Numerical simulation of the large-scale North American monsoon water sources. *J. Geophys. Res.,* **108,** 8614, doi:10.1029/2002JD003095.

Burde, G. I., 2006: Bulk recycling models with incomplete vertical mixing. Part I: Conceptual framework and models. *J. Climate,* **19,** 1461–1472.

CEC, 1997: Ecological regions of North America. Commission for Environmental Cooperation, Montreal, Canada, 71 pp.

Dominguez, F., and P. Kumar, 2008: Precipitation recycling variability and ecoclimatological stability—A study using NARR data. Part I: Central U.S. plains ecoregion. *J. Climate,* **21,** 5165–5186.

——, ——, X. Liang, and M. Ting, 2006: Impact of atmospheric moisture storage on precipitation recycling. *J. Climate,* **19,** 1513–1530.

Douglas, A. V., and P. J. Englehart, 1996: An analysis of the starting date for the summer monsoon in western Mexico and southeast Arizona. *Proc. 20th Annual Climate Diagnostics Workshop,* Seattle, WA, U.S. Department of Commerce, NOAA, 207–211.

Douglas, M. W., R. A. Maddox, and K. Howard, 1993: The Mexican monsoon. *J. Climate,* **6,** 1665–1677.

Eltahir, E., 1998: A soil moisture-rainfall feedback mechanism 1. Theory and observations. *Water Resour. Res.,* **31,** 765–776.

Gutzler, D. S., 2004: An index of interannual precipitation vari-

ability in the core of the North American monsoon region. *J. Climate,* **17,** 4473–4480.

——, and J. W. Preston, 1997: Evidence for a relationship between spring snow cover in North America and summer rainfall in New Mexico. *Geophys. Res. Lett.,* **24,** 2207–2210.

Higgins, R. W., and K. C. Mo, 1998: Interannual variability of the U.S. summer precipitation regime with emphasis on the southwestern monsoon. *J. Climate,* **11,** 2582–2606.

——, and Coauthors, 2003: Progress in pan American CLIVAR research: The North American Monsoon System. *Atmósfera,* **16,** 30–65.

Higgins, W., and D. Gochis, 2007: Synthesis of results from the North American Monsoon Experiment (NAME) process study. *J. Climate,* **20,** 1601–1607.

Koster, R., and Coauthors, 2004: Regions of strong coupling between soil moisture and precipitation. *Science,* **305,** 1138–1140.

Magaña, V., J. Amador, and S. Medina, 1999: The midsummer drought over Mexico and Central America. *J. Climate,* **12,** 1577–1588.

Masera, O., M. Ordonez, and R. Dirzo, 1997: Carbon emissions from Mexican forests: Current situation and long-term scenarios. *Climatic Change,* **35,** 265–295.

Mesinger, F., and Coauthors, 2006: North American Regional Reanalysis. *Bull. Amer. Meteor. Soc.,* **87,** 343–360.

Nigam, S., and A. Ruiz-Barradas, 2006: Seasonal hydroclimate variability over North America in global and regional reanalyses and AMIP simulations: Varied representation. *J. Climate,* **19,** 815–837.

Schmitz, J. T., and S. L. Mullen, 1996: Water vapor transport associated with the summertime North American Monsoon as depicted by ECMWF analyses. *J. Climate,* **9,** 1621–1634.

Small, E. E., 2001: The influence of soil moisture anomalies on variability of the North American monsoon system. *Geophys. Res. Lett.,* **28,** 139–142.

Stensrud, D. J., R. L. Gall, S. L. Mullen, and K. W. Howard, 1995: Model climatology of the Mexican monsoon. *J. Climate,* **8,** 1775–1794.

Tang, M., and E. R. Reiter, 1984: Plateau monsoons of the Northern Hemisphere: A comparison between North America and Tibet. *Mon. Wea. Rev.,* **112,** 617–637.

Trejo, I., and R. Dirzo, 2000: Deforestation of seasonally dry tropical forest: A national and local analysis in Mexico. *Biodivers. Conserv.,* **94,** 133–142.

Tucker, C., J. Pinzon, M. Brown, D. Slayback, E. Pak, R. Mahoney, E. Vermote, and N. ElSaleous, 2005: An extended AVHRR 8-km NDVI dataset compatible with MODIS and SPOT vegetation NDVI data. *Int. J. Remote Sens.,* **26,** 4485–4498.

Vivoni, E., and Coauthors, 2007: Variation of hydrometeorological conditions along a topographic transect in northwestern Mexico during the North American monsoon. *J. Climate,* **20,** 1792–1809.

Warner, T. T., 2004: *Desert Meteorology*. Cambridge University Press, 595 pp.

Watts, C. J., R. Scott, J. Garatuza-Payan, J. C. Rodriguez, J. H. Prueger, W. P. Kustas, and M. Douglas, 2007: Changes in vegetation condition and surface fluxes during NAME 2004. *J. Climate,* **20,** 1810–1820.

Xu, J., X. Gao, J. Shuttleworth, S. Sorooshian, and E. Small, 2004: Model climatology of the North American monsoon onset period during 1980–2001. *J. Climate,* **17,** 3892–3906.

Zeng, X., and E. Lu, 2004: Globally unified monsoon onset and retreat indexes. *J. Climate,* **17,** 2241–2248.